# Zn-doped GaSb epitaxial film absorption coefficients at terahertz frequencies and detector applications

Z. G. Hu and A. G. U. Perera[a)]
*Department of Physics and Astronomy, Georgia State University, Atlanta, Georgia 30303*

Y. Paltiel, A. Raizman, and A. Sher
*Electro-Optics Division, Soreq Nuclear Research Center (NRC), Yavne 81800, Israel*

(Received 4 March 2005; accepted 24 May 2005; published online 21 July 2005)

The reflectance measurements of *p*-type GaSb:Zn epitaxial films with different hole concentrations, grown by metalorganic vapor-phase epitaxy, have been investigated in the 3–30-THz frequency region. The experimental spectra were fitted using a classical harmonic Lorentz oscillator and the Drude model, illustrating that the hole effective mass and the mobility change with the carrier concentration. The hole effective mass was found to vary from $0.22m_0$ to $0.41m_0$ as the carrier concentration changed from $3.5\times10^{17}$ to $3.8\times10^{18}$ cm$^{-3}$. The mobility values derived from the reflectance measurements were slightly smaller than the values obtained from Hall-effect measurements. A sublinear relationship between the absorption coefficient and the hole concentration was found at a frequency of 3 THz. Those results can be used for designing GaSb-based terahertz detectors. © *2005 American Institute of Physics*. [DOI: 10.1063/1.1977195]

## I. INTRODUCTION

Among III-V compound semiconductors, gallium antimonide (GaSb) is particularly interesting for terahertz (THz) detection applications (i.e., 1 THz=300 $\mu$m).[1] The small band-gap energy together with the possibility of using the ternary compositions of InGaSb and InAsSb on a GaSb substrate makes GaSb a good candidate for far-infrared or terahertz detections. The optical and lattice vibration properties of GaSb bulk material have been investigated for several decades.[2–4] The recent progress in the film growth techniques, such as metalorganic vapor-phase epitaxy (MOVPE) and molecular-beam epitaxy (MBE), makes it possible to study the optical properties of GaSb epitaxial films.

In recent years, internal photoemission terahertz detectors based on Si or GaAs/AlGaAs material have been presented.[5,6] Those detectors are of high performance and present a threshold frequency as high as 2.3 THz. The detection mechanism in those detectors mainly involves free-carrier absorption in the heavily doped emitter layers, followed by the internal photoemission of photoexcited carriers across the junction barrier. Therefore, it is crucial to study the free-carrier absorption in order to improve the design of these detector structures.

The interaction of free carriers with photons in the terahertz-frequency region is one of the main parameters needed for optoelectronic device designs.[7] Recently, the free-hole absorption of $Al_xGa_{1-x}As$ epitaxial films were used to develop high-quality AlGaAs/GaAs terahertz detectors.[6,8,9] Due to a larger high-frequency dielectric constant and lower band-gap energy, GaSb epilayers should have a higher free-carrier absorption compared with GaAs epilayers. However, no free-hole absorption measurements for the GaSb epitaxial films were available in the literature.

Undoped GaSb is inheritably *p*-type irrespective of growth techniques and conditions.[4] Therefore, Hall-effect measurements of *p*-doped epilayers on the *p*-type substrate are hard to achieve. In addition, the doped substrate demonstrates large free-carrier absorption and negligible transmittance at low frequencies, preventing the use of transmittance measurements to determine the absorption coefficient.[7,10,11] Reflectance measurements, on the other hand, are still suitable for characterizing the optical properties of thin-film layers.[12] Moreover, the reflectance properties of the GaSb epilayers may also play an important role in designing resonant-cavity architectures for terahertz detectors.[13]

In this article, the 3–30-THz (10–100 $\mu$m) optical properties of *p*-type GaSb:Zn epitaxial films with different hole concentrations are investigated using near-normal-incident reflectance spectra. A theoretical model is presented to explain the experimental reflectance data. The fitted results are compared to the Hall-effect measurements done on *p*-type epilayers grown on *n*-type GaSb substrates. The effects of the hole concentration on the effective mass, mobility, and absorption coefficient will be discussed.

## II. EXPERIMENTS

GaSb epitaxial films were grown on GaSb substrates at a temperature of 600 °C and a reactor pressure of 400 Torr by MOVPE deposition technique. The epilayers were deposited using a Thomas Swan vertical reactor. Conventional trimethylgallium (TMGa) and trimethylantimony (TMSb) were used as precursors. The GaSb films were Zn-doped using zinc with diethylzinc as a dopant source and exhibited *p*-type conductivity. The growth rate was ~2 $\mu$m/h and the film thickness was 1.3 $\mu$m.

The *p*-type epilayers were grown simultaneously on both *p*- and *n*-type GaSb substrates. The *p*-type substrates were used for the reflectance measurements, while *n*-type sub-

a)Electronic mail: uperera@gsu.edu

 

strates were for the Hall-effect measurements. Reliable Hall results at room temperature were measured as the *p-n* junction was found to be efficient in electrically isolating the *p*-type epilayer from the *n*-type substrate.

Terahertz reflectance spectra for five GaSb epilayers were measured at room temperature over the frequency range of 3–30 THz (i.e., 100–1000 $cm^{-1}$) using a nitrogen-purged Perkin-Elmer system 2000 Fourier transform infrared (FTIR) spectrometer. Those measurements were compared to the reflectance spectrum of the one-side-polished GaSb substrate. The reflectance measurements were recorded at near-normal-incident configuration (the angle of incidence is 8°) using spectral reflectance accessory (Graseby Specac). For the high-frequency region of 450–1000 $cm^{-1}$, a liquid nitrogen-cooled mercury cadmium telluride (MCT) detector and an optimized KBr beamsplitter were used with a resolution of 4 $cm^{-1}$. A TGS/POLY detector and 6-$\mu$m-thick mylar beamsplitter were employed for the measurements in the low-frequency region of 100–700 $cm^{-1}$ with a resolution of 2 $cm^{-1}$. Aluminum (Al) and gold (Au) mirrors, the absolute reflectances of which were directly measured, were used as references for the reflectance spectra in the low- and high-frequency regions, respectively. The reflectance spectra from the two regions agree well within an experimental uncertainty of 5% inside the overlapped frequency region of 450–550 $cm^{-1}$.

## III. RESULTS AND DISCUSSION

A three-phase model (air/film/substrate) was used to calculate the reflectance spectra of the GaSb epitaxial films. At near-normal-incidence configuration, the following form describes the reflectance coefficient $r$:[14]

$$r = \frac{r_{01} + r_{12}e^{-i\delta}}{1 + r_{01}r_{12}e^{-i\delta}}, \tag{1}$$

where the partial reflectance coefficient $r_{01}$ (vacuum-film) and $r_{12}$ (film-substrate) are written as

$$r_{i(i+1)} = \frac{\sqrt{\varepsilon_i} - \sqrt{\varepsilon_{i+1}}}{\sqrt{\varepsilon_i} + \sqrt{\varepsilon_{i+1}}}, \tag{2}$$

and the phase factor for the film with thickness $d$ is described by the equation

$$\delta = \frac{4\pi d\sqrt{\varepsilon_1}}{\lambda}, \tag{3}$$

where $\lambda$ is the incident wavelength and the dielectric functions of vacuum, the film, and the substrate are $\varepsilon_0(=1)$, $\varepsilon_1$, and $\varepsilon_2$, respectively.

Thus, the reflectance $R$ is:

$$R = rr^*, \tag{4}$$

where the multireflections from the substrate could be neglected since the substrate was not polished on the back side. The experimental reflectance for the substrate did not contain any oscillation due to interference and this justifies the above assumption. The dielectric function of the substrate could be obtained, measuring the reflectance $R_s$ of the GaSb substrate using the known equation

$$R_s = \left| \frac{\sqrt{\varepsilon_2} - 1}{\sqrt{\varepsilon_2} + 1} \right|^2. \tag{5}$$

For polar semiconductor materials, the dielectric response can be described by the harmonic Lorentz oscillator model. The contribution from the free carriers to the dielectric function for doped semiconductors is commonly written in the classical Drude model. In order to describe *p*-type semiconductors heavy and light holes should be considered. However, in order to reduce the fitting parameters, an average effective value for the hole masses is considered. Therefore, the dielectric function $\varepsilon$ ($\varepsilon_1$ or $\varepsilon_2$) of the GaSb epitaxial films and the substrate can be written as

$$\varepsilon = \varepsilon_\infty \left( 1 - \frac{\omega_p^2}{\omega^2 + i\omega\gamma} \right) + \frac{S\omega_{\mathrm{TO}}^2}{\omega_{\mathrm{TO}}^2 - \omega^2 - i\omega\Gamma}. \tag{6}$$

Here, $\varepsilon_\infty$, $\omega_{\mathrm{TO}}$, $S$, $\Gamma$, $\omega_p$, and $\gamma$ represent the high-frequency dielectric constants, transverse-optical (TO)-phonon frequency, the oscillator strength, the broadening value of TO phonon, the plasma frequency, and the damping constant, respectively. The plasma frequency $\omega_p$ and the mobility $\mu$ of the free carrier are given by the following equations:

$$\omega_p = \sqrt{\frac{pq^2}{\varepsilon_o \varepsilon_\infty m_h^*}} \tag{7}$$

and

$$\mu = \frac{q}{2\pi c m_h^* \gamma}, \tag{8}$$

where $m_h^*$ is the average hole effective mass, $p$ is the carrier concentration, $q$ is the electron charge, and $\varepsilon_o$ is the vacuum permittivity.

Using a Levenberg-Marquardt algorithm, which is an efficient nonlinear calculation method for many parameter model,[15] the best-fit parameter values were found from Eq. (6). The fitting algorithm includes two main steps. First, the reflectance spectrum from the GaSb substrate was fitted to Eq. (6), whereas in the second stage those fitting parameters were used for modeling the reflectance spectra of the GaSb epilayers to obtain the absorption coefficient at different hole concentrations. Figure 1 displays the reflectance spectra from the substrate and the different epilayers. The results of the substrate reflectance fitting are listed in Table I. The high-frequency dielectric constant was found to be $15.1 \pm 0.1$, which is slightly higher than the reported value (14.5).[2] The TO and longitudinal-optical (LO)-phonon frequencies were found to be 226.4 and 236.4 $cm^{-1}$ [$\omega_{\mathrm{LO}}^2 = (S/\varepsilon_\infty + 1)\omega_{\mathrm{TO}}^2$], respectively, which are close to the previously measured values.[2] More importantly, the free-hole plasma frequency for the *p*-type GaSb substrate with low doping was given within the precision of 5% ($59.6 \pm 2.6$ $cm^{-1}$). Figure 2 shows the dielectric function of the GaSb substrate obtained from the reflectance spectrum. Those results are found to resemble the previous reports[16] at high frequencies above the TO-phonon frequency (6.8 THz). However, the imaginary part $\varepsilon_2$ is larger due to the free-carrier absorption at low frequencies (inset in Fig. 2).

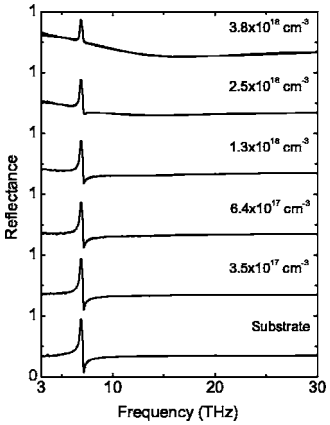


FIG. 1. Experimental reflectance spectra (dotted lines) of the GaSb substrate and films for different hole concentrations. The best-fit results are presented with solid lines. To distinguish between the results, each spectrum is successively shifted vertically by 1.0.

TABLE I. GaSb *p*-type substrate, reflectance spectra best-fit parameters. The errors give the 90% confidence limits. The high-frequency dielectric constant $\varepsilon_\infty$ and the oscillator strength $S$ is dimensionless, all the other parameters are in the unit of $cm^{-1}$.

| | | |
|---|---|---|
| $\varepsilon_\infty$ | High-frequency dielectric constant | 15.1±0.1 |
| $S$ | Oscillator strength | 1.36±0.02 |
| $\omega_{TO}$ | TO-phonon frequency | 226.4±0.1 |
| $\Gamma$ | TO-phonon broadening | 1.96±0.06 |
| $\omega_p$ | Plasma frequency | 59.6±2.6 |
| $\gamma$ | Damping constant | 73.3±5.0 |

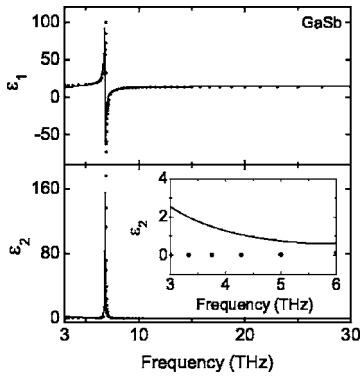


FIG. 2. The dielectric function of the *p*-type GaSb substrate was determined from the reflectance spectrum. The solid line is presenting the experimental results while for comparison the dotted line is showing Ref. 16 results. The inset gives a zoom for the frequency region of 3–6 THz.

In order to obtain the plasma frequencies and the damping constants of the GaSb epilayers, the values in Table I were used to fit the reflectance spectra to the Drude part of Eq. (6). Figure 1 displays the superposition of the theoretically calculated reflection spectra (solid lines) on the experimental results (dotted lines). An excellent agreement between the experimental and the calculated reflectance spectra was obtained in the entire frequency region. The clear peak observed in all spectra at 6.8 THz is assigned to the GaSb TO-phonon mode. With increasing hole concentration, the reflectance at low frequencies increases rapidly. A broad reflectance minimum can be identified in the two highest hole concentration spectra. In particular, for the film with the hole concentration of $3.8\times10^{18}$ $cm^{-3}$, the broad reflectance minimum appears near 13.5 THz. This minimum is a plasmon feature corresponding to the hole plasmon in *p*-type GaSb epilayer. The coupling interaction between the free-carrier plasmon and the LO-phonon mode is strongly affecting the shape of the phonon band, while the position of the phonon mode remains constant. The strongest effect can be identified when the plasma frequency is near the LO-phonon frequency. Accordingly, at low hole concentration, the phonon band is sharp and its peak is strong. With increasing hole concentration, the phonon band is broadened and its intensity decreases. These characteristics are similar to the reflectance spectra of *p*-type GaAs epilayers reported by Songprakob *et al.*[17] The theoretical calculations were able to reproduce all of those features including the broad reflectance minima.

As expected, the plasma frequency $\omega_p$ increases with the hole concentration. However, the damping constant $\gamma$ has a minimum ($49\pm4$ $cm^{-1}$) at the hole concentration of $6.4\times10^{17}$ $cm^{-3}$. This minimum indicates that the hole mobility at this doping concentration reaches its highest point. Generally, the hole concentration and the mobility are calculated using Eqs. (7) and (8) if the effective-mass and high-frequency dielectric constants are known. Similarly the effective mass and the mobility can be calculated using the hole concentration obtained from the Hall-effect measurements. The present hole mobility values for the GaSb epilayers from the Hall-effect and reflectance measurements are slightly below the reported data for the bulk materials in Ref. 18. The comparison between the Hall mobility ($\mu_{Hall}$) and the optical mobility ($\mu_{IR}$) is presented in Table II. The fitting errors of sample R509 with the lowest hole concentration are the largest due to stronger parameter correlations between the plasma frequency and the damping constant. Figure 3 displays the results graphically and shows the optical mobil-

TABLE II. GaSb *p*-type epitaxial films, reflectance spectra best-fit parameters. The plasma frequencies and the free-carrier damping constants were obtained from the model calculations. The errors give the 90% confidence limits. The hole concentration $p$ was determined from the Hall-effect measurements. The mobility was compared between the optical mobility ($\mu_{IR}$) and the Hall mobility ($\mu_{Hall}$) measurements.

| Sample | $p$ ($10^{17}$ $cm^{-3}$) | $\omega_p$ ($cm^{-1}$) | $\gamma$ ($cm^{-1}$) | $\mu_{IR}$ [$cm^2/(V\,s)$] | $\mu_{Hall}$ [$cm^2/(V\,s)$] |
|---|---|---|---|---|---|
| R509 | 3.5 | 90±3 | 116±11 | 313 | 410 |
| R514 | 6.4 | 106±3 | 49±4 | 552 | 390 |
| R513 | 13 | 138±1 | 114±5 | 199 | 280 |
| R512 | 25 | 222±1 | 194±5 | 164 | 200 |
| R511 | 38 | 317±2 | 226±6 | 190 | 260 |

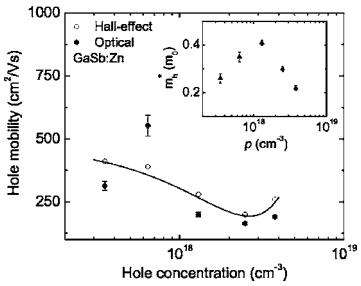


FIG. 3. The GaSb Hall mobility (○) compared with the optical mobility (●) for different hole concentrations. The two measurements follow a general trend, but in most cases the Hall mobility is slightly higher. The solid line shows the trend to guide the eyes. The inset shows the dependence of the effective mass for the GaSb epitaxial films on the hole concentration.

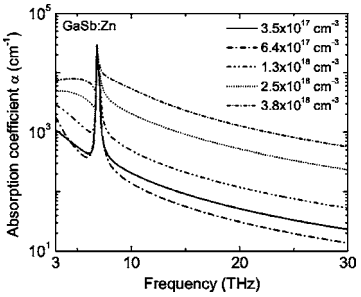


FIG. 4. Different hole concentrations and absorption coefficient variation of the GaSb epitaxial films at the frequency region of 3–30 THz.

ity calculated from the reflectance measurements together with the Hall mobility for different hole concentrations. In most cases, the Hall mobility appears to be slightly larger than the optical mobility, and $\mu_{\mathrm{Hall}}/\mu_{\mathrm{IR}}=1.23$ for the average value. Nevertheless, a reasonable agreement between the two types of measurements is seen and both measurements follow the same general trend. The sample R514 with the hole concentration of $6.4\times10^{17}$ cm$^{-3}$ is behaving differently. At this doping concentration the optical mobility is larger than the Hall mobility. Both measurements, however, indicate that this doping provides a peak in the mobility. The discrepancy between Hall-effect and optical reflectance analyses has been seen previously for *p*-type GaAs films and the average $\mu_{\mathrm{Hall}}/\mu_{\mathrm{IR}}$ ratio was reported to be from 1.5 to 3.7.[17,19] The difference indicates that the hole scattering time $\tau(=1/2\pi c\gamma)$ at terahertz frequencies is significantly smaller than the scattering time in direct current (dc) fields. The simplified Drude form used in Eq. (6), which considers only the statistical value of the damping constant not for the full Drude item, could be the major cause of the discrepancy.[17] A more rigorous theory would take into account the average carrier-energy distribution at each terahertz frequency. The approach is very complicated and the present simple approximation can give the effective reasonable results.[20] Further theoretical calculation which would give a more reasonable way of calculating the mobility is a topic for future studies.

The inset of Fig. 3 demonstrates the change in the effective mass with the hole concentration. A strong carrier concentration dependence was found and the hole effective-mass values vary from $0.22m_0$ to $0.41m_0$, where $m_0$ is the mass of the free electron. The values obtained are close to the value $(0.28\pm0.13)m_0$ for the GaSb bulk material with the hole concentration of $1.2\times10^{17}$ cm$^{-3}$ reported by Heller and Hamerly.[21] The calculated dependence of the hole effective mass on the carrier concentration could be found in the literature for $Ge_xSi_{1-x}$ and III-V semiconductors.[22,23] Since all the measurements were carried out at room temperature the hole effective mass was assumed to depend only on the Fermi level. Correspondingly, the Fermi level is a strong function of the carrier concentration. The theoretical calculations indicate that the shift of the Fermi level at room temperature is about 40 meV for *p*-type $Ge_xSi_{1-x}$ material with the carrier concentration of about $10^{18}$ cm$^{-3}$.[22] This large shift induces the variation of the hole effective mass. Due to the complex structure of the valence bands (the heavy-hole, light-hole, and spin split-off bands) for III-V semiconductors, hole effective masses deduced from the carrier concentration measurements appear to change with the physical properties studied.[21] This results in the discrepancy in the hole effective mass for different experimental methods. In addition, the hole effective mass also depends on the crystallographic orientation.[23] As a consequence, the small discrepancies in the orientation for the GaSb epilayers can also contribute to the different hole effective masses.

The absorption coefficient is one of the important factors for designing terahertz detectors. The calculated absorption coefficient is shown in Fig. 4. Below the TO-phonon frequency region, the absorption coefficient increases with the hole concentration due to the major contributions from the free-carrier absorption. It is interesting to note that at high frequencies the absorption coefficient of the GaSb epilayer with the hole concentration of $6.4\times10^{17}$ cm$^{-3}$ is smaller than that of the epilayer with the hole concentration of $3.5\times10^{17}$ cm$^{-3}$. This result may be ascribed to the smallest carrier damping constant for the former (sample R514).

The shift of the absorption coefficient at a frequency of 3 THz (100 $\mu$m) is shown in Fig. 5. This frequency is frequently used as the threshold frequency for terahertz detector design. The terahertz absorption coefficient of the GaSb epitaxial films can be empirically fitted to the following relationship:

$$\alpha_3 = 9.7\times10^{-12}p^{0.80}. \tag{9}$$

Here, $p$ is the hole concentration. As expected, Eq. (9) shows a sublinear increase of the absorption coefficient with the carrier concentration, which indicates that increasing the

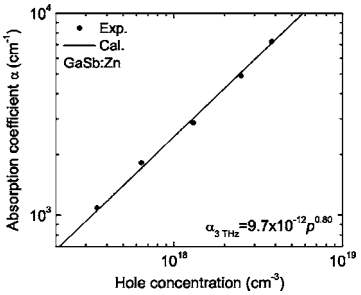


FIG. 5. Sublinear relationship between the hole concentration and the absorption coefficient of the GaSb epitaxial films at the frequency of 3 THz (100 $\mu$m).

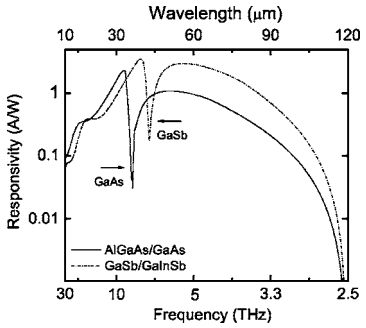


FIG. 6. The calculated responsivity of terahertz detectors using AlGaAs/GaAs and GaSb/GaInSb material systems at an applied field of 1.0 kV/cm. The structure parameters could be found in Ref. 6 except for the carrier concentration of $2.5\times10^{18}$ cm$^{-3}$ for the emitter/absorber. The arrows indicate the TO-phonon modes of the GaAs and GaSb, respectively.

hole concentration can improve the terahertz absorption in the emitter/absorber of the detectors.[6] The present work indicates that the absorption coefficient is about $4.9\times10^{3}$ cm$^{-1}$ for the GaSb epilayer with the hole concentration of $2.5\times10^{18}$ cm$^{-3}$. This value is higher than that for AlGaAs film with a similar concentration.[8]

Figure 6 shows a comparison of the calculated responsivity for terahertz detectors based on GaAs and GaSb material systems using the fitting parameters. The HEIWEP detector structure, which contains ten periods of $2.5\times10^{18}$ cm$^{-3}$, 500-Å-thick emitter/absorber, and 2000-Å-thick barrier sandwiched between two contacts, is the same as the previous design in Ref. 6 The responsivity of the GaSb-based detector is higher than that of the GaAs-based detector at low terahertz frequencies. This indicates that the absorption of the GaSb-based detector is larger due to a higher absorption coefficient of the *p*-type GaSb epilayer. The spectral responsivity is inherently broadband since both the initial and final carrier states are part of the same continuum for the free-hole absorption. The calculated peak responsivity (3.0 A/W) of GaSb-based detector is larger by a factor of three than that of GaAs-based detector (1.0 A/W) at an applied field of 1.0 kV/cm. Therefore, the *p*-type GaSb epilayers should be better candidates for designing high-quality terahertz detectors. Moreover, using GaSb layers with low hole concentrations as the emitters of terahertz detectors could decrease the dark current and further improve the signal-to-noise ratio.

## IV. CONCLUSIONS

The reflectance measurements of *p*-type GaSb:Zn epitaxial films with different hole concentrations have been investigated in the terahertz-frequency region of 3–30 THz. The hole effective mass shows a strong dependence on the hole concentration. The plasma frequency and free-carrier damping constant increase with the hole concentration. The calculated results indicate that the absorption coefficient increases with the hole concentration in the low-frequency region. An important sublinear relationship between the absorption coefficient and the hole concentration is observed and found to be higher than that for the previously used GaAs system. Those results suggest the GaSb system as a good candidate for utilizing efficient high-quality terahertz detectors.

## ACKNOWLEDGMENTS

The work was supported in part by the U.S. NSF under Grant No. ECS-0140434. The authors would like to acknowledge Dr. S. G. Matsik, M. B. M. Rinzan, and G. Ariyawansa for many fruitful discussions and technical support.

[1] P. S. Dutta, H. L. Bhat, and V. Kumar, J. Appl. Phys. **81**, 5821 (1997).
[2] M. Hass and B. W. Henvis, J. Phys. Chem. Solids **23**, 1099 (1962).
[3] S. Zollner, M. Garriga, J. Humlek, S. Gopalan, and M. Cardona, Phys. Rev. B **43**, 4349 (1991).
[4] R. Pino, Y. Ko, and P. S. Dutta, J. Appl. Phys. **96**, 1064 (2004).
[5] A. G. U. Perera, W. Z. Shen, S. G. Matsik, H. C. Liu, M. Buchanan, M. O. Tanner, and K. L. Wang, Appl. Phys. Lett. **72**, 2307 (1998).
[6] M. B. M. Rinzan, A. G. U. Perera, S. G. Matsik, H. C. Liu, Z. R. Wasilewski, and M. Buchanan, Appl. Phys. Lett. **86**, 071112 (2005).
[7] S. K. Ray, T. N. Adam, R. T. Troeger, J. Kolodzey, G. Looney, and A. Rosen, J. Appl. Phys. **95**, 5301 (2004).
[8] M. B. M. Rinzan, D. G. Esaev, A. G. U. Perera, S. G. Matsik, G. Von Winckel, A. Stintz, and S. Krishna, Appl. Phys. Lett. **85**, 5236 (2004).
[9] Z. G. Hu, M. B. M. Rinzan, S. G. Matsik, A. G. U. Perera, G. Von Winckel, A. Stintz, and S. Krishna, J. Appl. Phys. (in press).
[10] W. Z. Shen, A. G. U. Perera, S. K. Gamage, H. X. Yuan, H. C. Liu, M. Buchanan, and W. J. Schaff, Infrared Phys. Technol. **38**, 133 (1997).
[11] A. G. U. Perera, W. Z. Shen, W. C. Mallard, M. O. Tanner, and K. L. Wang, Appl. Phys. Lett. **71**, 515 (1997).
[12] R. Ferrinia, M. Patrini, and S. Franchi, J. Appl. Phys. **84**, 4517 (1998).
[13] D. G. Esaev, M. B. M. Rinzan, S. G. Matsik, and A. G. U. Perera, J. Appl. Phys. **96**, 4588 (2004).
[14] O. S. Heaven, *Optical Properties of Thin Solid Films* (Dover, New York, 1991).
[15] W. H. Press, S. A. Teukolsky, W. T. Vetterling, and B. P. Flannery, *Numerical Recipes in C: The Art of Scientific Computing* (Cambridge University Press, Cambridge, MA, 1992).
[16] D. F. Edwards and R. H. White, *Handbook of Optical Constants of Solids II*, edited by E. D. Palik (Academic, New York, 1991).
[17] W. Songprakob, R. Zallen, W. K. Liu, and K. L. Bacher, Phys. Rev. B **62**, 4501 (2000).
[18] J. D. Wiley, *Semiconductors and Semimetals*, edited by R. K. Willardson and A. C. Beer (Academic, New York, 1975), Vol. 10.
[19] G. Irmer, M. Wenzel, and J. Monecke, Phys. Rev. B **56**, 9524 (1997).
[20] H. A. Lyden, Phys. Rev. **134**, A1106 (1964).
[21] M. W. Heller and R. G. Hamerly, J. Appl. Phys. **57**, 4626 (1985).
[22] Y. Fu, S. C. Jain, M. Willander, and J. J. Loferski, J. Appl. Phys. **74**, 402 (1993).
[23] R. H. Henderson and E. Towe, J. Appl. Phys. **79**, 2029 (1996).